Published in final edited form as:
Neuroimage. 2012 January 16; 59(2): 1896–1903. doi:10.1016/j.neuroimage.2011.08.088.

Joint ICA of ERP and fMRI during Error-Monitoring

Bethany G. Edwards[1], **Vince D. Calhoun**[1,2], and **Kent A. Kiehl**[1,3,4,*]

[1]The Mind Research Network, Albuquerque, NM, USA

[2]Department of ECE, University of New Mexico, Albuquerque, NM, USA

[3]Department of Psychology, University of New Mexico, Albuquerque, NM, USA

[4]Department of Neuroscience, University of New Mexico, Albuquerque, NM, USA

Abstract

The anterior cingulate cortex (ACC) is commonly separated into two functional divisions: the cognitive division, which lies in the caudal region and the affective division, which lies in the rostral region of the ACC. Both regions of the ACC are engaged during error-monitoring tasks; however, little is known about the temporal sequencing associated with cognition and affective processes during error-monitoring. Here we use joint Independent Component Analysis (jICA) to couple event-related potential (ERP) time courses and functional magnetic resonance imaging (fMRI) spatial maps to examine the spatio-temporal stages of engagement in the two divisions of the ACC during error-monitoring. Consistent with hypotheses, two of the five significant spatio-temporal components identified by jICA revealed that the error-related negativity (ERN) ERP was associated with distinct spatial fMRI patterns in the ACC. The ERN_1 was associated with activity in the caudal ACC and lateral prefrontal cortex (lPFC) while the ERN_2 was associated with activity in the rostral ACC. These results suggest that during error-monitoring the caudal ACC and lPFC engage prior to the rostral ACC. These results suggest that cognition precedes affect during error-monitoring.

Keywords

Event-related potential; fMRI; independent component analysis; anterior cingulate; lateral prefrontal cortex

1. Introduction

The anterior cingulate cortex (ACC) has been shown to be involved in a variety of processes including those with cognitive and affective components. The ACC has been implicated as a central part of a system involved in the regulation of behavior and in both conflict and error processing (Badgaiyan, 1998; Dehaene, 1994; Garavan, 2003; Kiehl, 2000; Logan, 1985; Shallice, 1988; Stuss, 1997). Prior research has suggested that the ACC may be more directly involved with the monitoring of response conflict rather than the monitoring of errors (Botvinick, 2001; Carter, 1998). More specifically, the ACC has been shown to be activated during a variety of tasks with high conflict response leading to competing response

Correspondence Kent A. Kiehl, Ph.D., Mind Research Network, 1101 Yale Blvd NE, Albuquerque, NM 87106, Phone: 505-925-4516, Fax: 505-272-8002, kkiehl@unm.edu.

Conflict of Interest Statement

The authors declare that the research was conducted in the absence of any commercial or financial relationships that could be construed as a potential conflict of interest.

tendencies, such that errors may occur when the incorrect response overwhelms the correct one (Botvinick, 2001; Carter, 1998; Swick, 2002). For example, the ACC has been shown to be activated when participants are required to divide their attention between stimuli, causing errors of interference (e.g. dual-monitoring task) (Corbetta et al., 1991). The ACC has also been shown to be activated in tasks requiring response inhibition or competition, such as the stroop task (leading to errors especially in the incongruent condition) (Barch et al., 2001; Carter et al., 2000), and in tasks where participants frequently make large numbers of errors (e.g. false alarms), such as the go/no-go task (Braver, 2001; Kiehl, 2000). In a go/no-go task, a series of target and distracter stimuli are presented and participants are asked to respond to target stimuli ("go") but not to distracter stimuli ("no-go"). In the task, there is a much higher probability that a target versus a distracter will appear; therefore, a strong stimulus-response mapping is established on "go" trials. When participants are then forced to refrain from responding on a "no-go" trial, response-related conflict arises since the correct response has to compete with the established stimulus-response pattern (Braver, 2001). A go/no-go task allows one to examine conflict and error processing as errors may be expected to happen on trials where there is strong response conflict. Prior research has suggested that there is a neuroanatomical separation for conflict and error processing. Garavan et al. (2003) had participants perform a go/no-go task in which they manipulated response conflict by using an on screen stimulus duration combined with instruction to respond during its presentation. They found anterior areas of the ACC to significantly respond to errors but not to the changing conflict demands of the task; therefore, providing evidence that error-related processes may be neuroanatomically distinct from conflict-monitoring processes (Garavan, 2003).

The ACC is commonly separated into two functional divisions: one cognitive and the other affective (for review see (Bush, 2000; Devinsky, 1995). The cognitive division of the ACC lies more caudal while the affective division lies more rostral. While these regions are commonly referred to as caudal and rostral ACC (Kiehl et al., 2000), the cognitive division has also be referred to as anterior midcingulate cortex (aMCC) and the rostral division as pregenual ACC (pACC) (Vogt, 2005). These two divisions seem to show differences in error and conflict-related activity during error trials, for example certain areas of the ACC may respond more to response-related conflict that may arise during a task rather than the actual processing of errors (Botvinick, 2001; Carter, 1998). The caudal ACC region seems to respond to the apparent conflict that arises during a "no-go" trial, therefore showing involvement in the detection of an error while the rostral ACC region seems to be involved in an affective response which may occur shortly after an error is made (Braver, 2001; Kiehl, 2000). As previously mentioned, Garavan et al. (2003) found the anterior portions of the ACC to be activated with errors during a go/no-go task but not with the conflict demands of the task, suggesting that this responsiveness to an error may reflect involvement in emotional processing. Error-processing may somehow be involved in the formation of an emotional response to an error, providing additional evidence toward a theoretical distinction between error-processing and conflict-monitoring functions (Garavan, 2003).

The caudal and rostral divisions of the ACC also appear to have specific connections with other areas of the brain. The rostral division has been found to have connections with several emotion-related areas (e.g. amygdala, hypothalamus, and insula) and tends to be involved in the evaluation of affective information and affective responses to errors (Devinsky, 1995; Drevets, 1998; Polli, 2009; Vogt, 1992; Whalen, 1998). The caudal division has been shown to have connections with the lateral prefrontal cortex (lPFC) and tends to be involved in processes including attention, interference, response competition, and error detection (Botvinick, 2004; Braver, 2001; Bush, 2000; Casey, 2000; Devinsky, 1995; Downar, 2002; Kiehl, 2000; Ruff, 2001). More specifically, it has been argued that the caudal ACC is involved in conflict and error detection (Botvinick, 2004; Braver, 2001; Carter, 1998; Kiehl,

2000; Ullsperger, 2001) while the lPFC is involved in the regulation of behavior in situations that involve response conflict (Botvinick, 2004; Bush, 2000; Carter, 1999; Devinsky, 1995). The current study uses multimodal neuroimaging measures to examine the temporal stages of engagement of the two divisions of the ACC during error-monitoring. In order to test our hypothesis that the cognition precedes that of the affect, we examine these interconnections and explore whether the caudal ACC and lPFC occur around the same time following an error response and, furthermore, whether they precede activation of the rostral ACC.

Numerous event-related potential (ERP) and functional magnetic resonance imaging (fMRI) studies have explored the issue of error-related brain activity in depth (Falkenstein, 1991; Gehring, 1990, 1993). ERP studies have shown that, following an incorrect action, a two-component action occurs starting with a negative deflection in the ERP (ERN) and followed by a positive deflection in the ERP (Pe) (Debener, 2005; Gehring, 1990; Hajcak, 2003; Herrmann, 2004). These two components are thought to be partly independent (Hajcak, 2003; Herrmann, 2004). When a participant makes an error during a cognitive task, the negative deflection in the event-related potential is thought to peak approximately 50 to 150 milliseconds after the incorrect response while the positive deflection is thought to peak approximately 200 to 400 milliseconds after the incorrect response (Debener, 2005; Falkenstein, 2000; Gehring, 1990; Nieuwenhuis, 2001). This negative deflection in the ERP (ERN) or error negativity (N_e) has been hypothesized to indicate that the response outcome unfulfilled participant expectations while the positive deflection in the ERP (Pe) has been hypothesized to be involved in additional processing that may occur after an error, processing that may be different than just detection of an error (Brown, 2005; Holroyd, 2004). Furthermore, Falkenstein (2000) suggests that this additional processing of the Pe is resonated in a P3 wave which is caused by a participant error. Previous research has indicated that the ERN and Pe both seem to have a medial frontal generator in the brain, possibly originating in the ACC (Dehaene, 1994; Gehring, 2001; Hajcak, 2005; Herrmann, 2004). Although there has been much evidence supporting a medial frontal generator, the specific divisions of the ACC and their exact roles in this process remain unclear.

A combination of source localization and fMRI studies have suggested that the ERN response generates in a rostral cingulate zone (RCZ), most likely located within the ACC and/or the supplementary motor area (SMA) (Dehaene, 1994; Roger, 2010; Ullsperger, 2001). More specifically, a previous fMRI study found the rostral ACC regions to be more sensitive to errors compared to baseline while a previous EEG study found the ERN response to be associated with activation in the rostral and dorsal ACC (Debener, 2005; Kiehl, 2000; Luu, 2003). The ERN may reflect an affective process that occurs directly after a participant makes an error such that they may evaluate their actual response (e.g. incorrect response) and the correct response, resulting in activation in certain parts of the brain associated with affective processing (Bernstein, 1995; Coles, 1998; Devinsky, 1995; Luu, 2003). To date, there has been little examination of the specific sequence of events occurring in the ACC and lPFC following the error response. Dissociating the generators of the ERN is complicated by the inverse problem and associated assumptions (Cohen, 1990; Srinivasan, 1999). To address these issues, the current study examines both the spatial and temporal dynamics of error and conflict processing in order to begin to understand these regions following acknowledged error commission. Joint independent-component analysis (jICA) (Calhoun, 2001; Debener, 2005) is employed to test our hypotheses regarding the spatio-temporal decoupling of the affect and cognition in the ACC and the ERN. Joint ICA is an analysis approach allowing for the combination of two modalities (fMRI and ERP) by pinpointing components of each modality and the connections that exist between the two (Calhoun, 2006, 2009). The BOLD response in the fMRI data is potentially too slow to catch the temporal dynamics needed to understand cognitive processes that may be

occurring while ERP data has the ability to capture very precise temporal information but has limited spatial resolution (Calhoun, 2006).

Using ICA to integrate fMRI and ERP data allows for the identification of when and where changes in the signal occur and to test the hypothesis that error processing occurs simultaneously in the lPFC and caudal ACC, and precedes error processing in the rostral ACC. That is, cognition may come before affective processing during error monitoring.

2. Material and Methods

2.1. Participants

Participants included 41 right-handed (18 male, 23 female) healthy participants (mean age = 33.34, standard deviation = 9.08) recruited from the Institute of Living/Hartford Hospital. All participants signed informed consent prior to their participation in the study and all experimental procedures were approved by the Institutional Review Board (IRB) at Hartford Hospital. Participants were screened to eliminate neurological and/or psychiatric problems. In addition, participants were excluded for psychosis in a first degree relative. Participants were paid $20/hour for their participation.

2.2. Stimuli and Task Procedures

For fMRI, stimuli were presented to study participants using a custom visual and auditory presentation package via a computer-controlled projection system that delivered a visual stimulus at a visual angle of ~3 × 3.5° to a rear-projection screen located at the rear entrance to the magnet bore. Participants viewed this screen using a system of mirrors attached to the top of the head coil. For ERP, the stimuli were presented on a LCD monitor. The visual angle for all stimuli was matched across fMRI and ERP presentation systems.

Participants performed a go/no-go task in which a series of Xs (target stimuli) and Ks (distracter stimuli) were shown (Kiehl, 2000). Participants were instructed to respond as quickly and accurately as possible with their right index finger every time the “X” (.80 probability) appeared and to not respond to the “K” (.20 probability). The stimuli were presented for 250 msec. The inter-stimulus interval between “X” stimuli (“go” stimuli) varied pseudo-randomly between 1000, 2000, and 3000 ms, subject to the constraint that in each consecutive six second period, three “X” stimuli were presented. The “K” stimuli were interspersed among the “X” stimuli in a pseudorandom manner subject to two constraints: the intervals between K stimuli were in the range 10 to15 s and these stimuli had equal probability of occurring at 0, 500, and 1000 ms after the beginning of a 1500 ms image acquisition period in fMRI. By varying the phase of the stimulus presentation relative to the acquisition time, we were able to effectively sample the hemodynamic response to the stimuli of interest uniformly at 500 ms intervals. A commercially available MRI compatible fiber optic response device (Lightwave Medical, Inc., Vancouver, B.C., Canada) was used to acquire behavioral responses. Reaction times were computed on trials for which the participant responded correctly within 1000 ms post-stimulus. Before entry into the scanning room, each participant performed a practice block of 10 trials to ensure understanding of the instructions.

2.3. fMRI

Functional MRI and ERP data were acquired in separate sessions occurring on the same day. Each session, consisting of the exact same task, were counterbalanced across participants. The fMRI data were acquired on a Siemens Allegra 3T dedicated head scanner equipped with 40 mT/m gradients and a standard quadrature head coil. The functional scans were acquired using gradient-echo echo-planar-imaging with the following parameters (TR =

1.5s, TE = 27ms, FOV=24cm, acquisition matrix = 64 × 64, flip angle = 70°, voxel size = 3.75 × 3.75 × 4 mm, gap = 1mm, 29 slices, ascending acquisition). The first six images in each BOLD run were used to allow the scanner to reach a steady state and were discarded. Following the first six images, the scanner automatically triggered the task paradigm to then begin.

Functional MRI data were preprocessed using the software package SPM2. Images were realigned using INRIalign, a motion correction algorithm unbiased by local signal changed (Freire, 2002). The data were then whole-brain normalized into standard Montreal Neurological Institute space (Friston, 1995) and spatially smoothed with a 12 × 12 × 12 mm full-width half-maximum Gaussian kernel.

2.4. Event-Related Potential Recording

The ERP data were collected using a 64 channel SA bioelectric amplifier system. Amplifiers were connected to a 16-bit A/D conversion using a custom program (digitize) implemented on a Pentium II microcomputer running a real-time kernel of Solaris for Intel. The digitize program recorded the continuous EEG data and all stimulus and behavioral response codes for subsequent analysis.

Tin electrodes (ElectroCap International) recorded scalp potentials across a total of 62 electrode sites. Placement of the electrodes was in accordance with the standard placement guidelines of the International 10 – 20 System, along with some additional sites. Vertical and horizontal electrooculograms (EOG) recordings were monopolar and were monitored from electrodes located on the lateral and supraorbital ridges of the right eye. All electrodes were referenced to the nose. Electrical impedances were maintained below 10 kΩ throughout (Dehaene, 1994) the experiment. The EEG channels (SA instruments) were amplified (20,000 gain) with a band pass of 0.01 to 100 Hz, digitized on-line at a rate of 500 samples/sec, and recorded on computer hard disk. EEG data were preprocessed using ICA to remove ocular artifacts from the EEG data (Jung, 2000). Data were then digitally filtered with a 20 Hz low pass filter to reduce electromyographic activity and ERPs were constructed for trials in which participants incorrectly responded to distracter stimuli. The recording epoch was 1400 ms long with a 200 ms pre-stimulus baseline. Data from a midline central site (Fcz) were included in the ICA fusion analyses because it was the channel at which the ERN was maximal (refer to supplemental material for response locked averages for false alarms and correct hits).

2.5. fMRI and ERP Data Fusion

Independent components were estimated by their input to the average ERP time course by regressing the components onto the average data and computing the maximum absolute peak of the fitted time courses. Components which contributed greater than 1 standard deviation to the average time course were extracted as this was reasonable criteria for removing components that did not have focal peaks and had more random looking time courses. Since the independent component results were calibrated directly from the original ERP data, the sign of the decomposition in turn reflects the sign of the ERP data.

We adopted the same method as shown in Calhoun et al. (2006). We computed spatiotemporal “snapshots” of the significant components in order to better understand how the joint components (shown in Fig. 2) interact with each other. We first computed a linear combination of the fMRI components weighted by their joint ERP time courses for a specific time point. The N spatial (fMRI) component is written as $S = [s_1 \ldots s_N]$, and the N temporal component (ERP) as $T = [t_1 \ldots t_N]$, where s_i is a $V \times 1$ vector containing the V brain voxels and t_i is a $T \times 1$ vector containing the ERP time points. We then computed the

fMRI movie as $M_F = |T| \times S^T$ (the absolute value is needed since the joint components are fused using a single weight parameter). Therefore, an amplitude change in the fMRI component is directly linked to a change in the ERP component. Likewise, we computed an estimated ERP time course for a given voxel by computing $M_E = T \times |S|^T$.

3. Results

3.1. Behavioral Results

Behavioral data were analyzed to ensure that there were no significant differences between the fMRI and EEG task data. Paired-sample t-tests were conducted to analyze task performance in terms of reaction time to hits and false alarms and percentage of false alarms (k or 'no-go' stimuli not followed by a button press within 1000ms), hits (x or 'go' stimuli followed by a button press within 1000ms), and correct rejects (k or 'no-go' stimuli not followed by a button press within 1000ms). Refer to Table 1 for a detailed summary of task performance in both sessions. Although participants did respond slightly slower to the task during the fMRI session for both hits and false alarms, there were no significant differences in reaction times across sessions (hits: $t(40) = 1.89$, $p = 0.07$; false alarms: $t(40) = 1.35$, $p = 0.19$). Participant task performance was slightly better during the EEG session compared to the fMRI session, with more correct rejects and hits and fewer false alarms; however, there were no significant differences in terms of task performance between the two sessions (correct rejects: $t(40) = -1.85$, $p = 0.07$; hits: $t(40) = -1.74$, $p = 0.09$; false alarms: $t(40) = 1.64$, $p = 0.11$).

3.2. fMRI and Event-Related Potential Results

To obtain results for the false alarm response, functional MRI data underwent a random effects analysis. The group fMRI data is displayed on a t-map thresholded at $p < 0.001$, corrected for multiple comparisons using the false discovery method, showing areas of positive activation for false alarms versus a 200 msec averaged pre-stimulus baseline. The fMRI map (shown in Figure 1A) demonstrates activation in areas commonly associated with affective processing, including the anterior cingulate, ventromedial prefrontal cortex, left lateral prefrontal cortex, and insula. ERP data was also averaged across participants to obtain an average ERP curve for false alarms versus the pre-stimulus baseline. The ERP graph (shown in Figure 1B) illustrates the average ERP response for false alarms versus pre-stimulus baseline across participants (bold yellow line), along with individual ERP components. As shown in prior ERP studies, a negative deflection in the response-locked average ERP response across participants occurs slightly after the error is made (Brown, 2005; Debener, 2005; Gehring, 1990; Holroyd, 2004).

As previously mentioned, joint ICA is an analysis approach allowing for the combination of two modalities (fMRI and ERP) by jointly maximizing the spatial independence of the fMRI data and the temporal independence of the ERP data while identifying linked components which show common inter-subject co-variation (Calhoun, 2006, 2009). By using joint ICA to examine the fMRI and ERP data simultaneously, we identified areas of the brain that were associated with portions of the time courses in the ERP data (Calhoun, 2006). Therefore, through joint estimation of spatial and temporal independence, we captured the variance and identified five significant spatio-temporal components that had an ERP waveform above flat baseline. In order to determine these significant spatio-temporal components, we fit all components (shown in Fig. 1B) to the average ERP waveform via regression and took the standard deviation of each component. Components with a standard deviation greater than one were interpreted as significant while those with a standard deviation less than one were not. Figure 2 delineates the five components (2A–E), showing spatial (fMRI) and temporal (ERP) dynamics of each component. In each figure,

"snapshots" of the fMRI maps are weighted by the ERP part of the components at specific points in time; therefore, showing significant regions of activation associated with each component at specific time points. ERP graphs are shown with the yellow line indicating the ERP time course averaged across subjects in yellow and the ERP time course specific to that component. Consistent with prior work, the jICA decomposition shown in Figure 2 shows two negative independent components (ERN_1 and ERN_2) and three positive independent components (Pe_1, Pe_2, & Pe_3) (Calhoun et al., 2006). By viewing the fMRI maps and ERP time course plots for each component simultaneously, we are able to identify specific brain regions that are associated with the distinct ERP time course components (Calhoun, 2006). The ERN_1 and ERN_2 components, shown in Figures 2A and 2B, are associated with significant activation in regions including the lPFC (ERN_1: left middle frontal gyrus, x, y, z = −36, 0, 66; right middle frontal gyrus, x, y, z = 45, 0, 54; ERN_2: left middle frontal gyrus, x, y, z = −33, 60, 3), and the anterior cingulate (ERN_1: caudal anterior cingulate, x, y, z = 0, 24, 27; x, y, z = 3, 27, 24 – ERN_2: rostral anterior cingulate x, y, z = −3, 42, −3; x, y, z = 0, 3, 0; x, y, z = 3, 6, −3). The two components are shown to be maximally independent. More specifically, the ERN_1 component (Figure 2A), occurring first at 48 msec, shows an association with activation in the caudal anterior cingulate while the ERN_2 component (Figure 2B), occurring second at 86 msec, shows an association with activation in the rostral anterior cingulate. Refer to Table 2 for a detailed summary of regions of the ACC that are engaged, showing selected MNI coordinates of the volume and maxima of each anatomic region within the maps (refer to supplementary material for a detailed summary of regions of both the ACC and lPFC that are engaged). We also briefly examined activity associated with the three positive ERP components. Each ERP component (Pe_1, Pe_2, Pe_3 in Figures 2C to 2E) is associated with the anterior cingulate, middle frontal gyrus and superior frontal gyrus. In regard to the ACC activation, the Pe_2 component is associated with negative activation in the caudal ACC while the Pe_3 component is associated with negative activation in the rostral ACC.

4. Discussion

4.1. Caudal ACC and lPFC Interactions in Error-Processing

In the current study, we explored the hypothesis that error processing occurs simultaneously in the lPFC and caudal ACC, and precedes error processing in the rostral ACC. In order to test this hypothesis, we examined the interconnections of the ACC and lPFC during a go/no-go task and explored the specific sequence of activation that occurs after an error is made. Prior research has provided evidence that the caudal division of the ACC has connections with the lPFC, showing involvement in processes including attention, interference, response competition, and error detection (Botvinick, 2004; Braver, 2001; Bush, 2000; Casey, 2000; Devinsky, 1995; Downar, 2002; Kiehl, 2000; Ruff, 2001). By using ICA in the current study, we were able to jointly analyze the fMRI and ERP data from our sample of participants in order to delineate spatial information from the BOLD data and temporal information from the ERP data. Directly after the error occurs, we see a negative deflection in the ERP as shown with ERN_1 and ERN_2 components. We were then able to delineate the fMRI activity associated with the ERN_1 and ERN_2 components through our jICA approach and found that, as predicted, the ERN_1 component was associated with hemodynamic activity in the caudal ACC and lPFC. This date provides additional evidence that the ACC and lPFC are indeed both engaged during error-processing.

Specifically, we found that the ERN_1 component (48 msec) occurred 38 msec earlier in time than the ERN_2 component (86 msec), showing that both the caudal ACC and lPFC occurred around the same time following an error. It may be that a post-error process similar to that suggested by Debener and colleagues may be occurring. Conflict may be occurring post-response between executed and activated response tendencies when an incorrect response

overwhelms the correct one, leading to an outcome that is worse than expected (Debener, 2005). During the go/no-go task, a stimulus-response mapping is established on 'go' trials since these trials occur the majority of the time. On a no-go trial, participants face response conflict and are sometimes unable to overcome the previously established stimulus-response mapping, therefore, making an error. With evidence that the lPFC and caudal ACC are both involved in response competition and error detection, we believe that when a participant makes an error on a no-go trial, the participant may undergo a *post-error* cognitive response between conflicting response tendencies via the caudal ACC and lPFC.

4.2. Activation of the ACC during Error-Processing

The current study has also provided additional evidence in regard to error-related differences between the caudal and rostral ACC during error trials. Prior research has shown that the caudal ACC responds to conflict that arises on a no-go trial while the rostral ACC is involved in an affective response to the error (Braver, 2001; Kiehl, 2000). In addition to finding that the caudal ACC and lPFC occur around the same time following an error, the latency differences between the two ERN components demonstrated that activation of both regions occurred prior to that of the rostral ACC, suggesting that the two divisions of the ACC indeed show differences in error-related activity during error trials (Carter, 1998). Through delineating spatial information associated with the ERN_1 and ERN_2 components we found that the ERN_2 component occurred 86 msec following the ERN_1 (or following the button press), showing an association with activation in the rostral ACC. While the caudal ACC seems to be involved in a cognitive response to the actual detection of an error, the rostral ACC may be involved in further processing, possibly emotional processing, that occurs in addition to just following error detection. Prior research has suggested that the rostral ACC region seems to be involved in an affective response which may occur shortly after an error is made. More specifically, after undergoing a post-error response dealing with conflicting response tendencies via the caudal ACC and lPFC, the participant may process that the outcome was worse than expected and form an emotional response to the error. Therefore, the participant may further evaluate his or her error by processing this affective information via the rostral ACC.

The current study also briefly examined the three significant positive components occurring after the initial negative ERP deflection following an error response. Prior research has shown that the positive component is associated with the rostral ACC, indicating involvement in post-error processing and, therefore, may reflect an affective response to an error (Hermann et al., 2004). Furthermore, Falkenstein and colleagues (2000) have suggested that the Pe component may reflect additional post-error processing that is independent from the ERN. More specifically, this post-error processing may be in the form of error recognition, response strategy adjustment, and/or affective error assessment (Falkenstein et al., 2000). Through ICA, we found there to be three positive independent components following an error response, each showing an association with the ACC. The Pe_1 component was associated with hemodynamic activity in both the caudal and rostral divisions; however, the Pe_2 and Pe_3 components showed distinct differences in ACC activity such that the Pe_2 was associated with activation in the caudal division while the Pe_3 was associated with activation in the rostral division. Our results seem to indicate, along with prior research, that these positive components may indeed reflect some sort of affective response via the rostral ACC when an error occurs; however, in addition they suggest the possibility of a cognitive response also occurring via the caudal ACC during post-error processing. Therefore, these positive components may be involved in both affective and cognitive processing following an error. One explanation for this sequence of activation is that dynamic coupling may be occurring over time, such that there may be multiple re-entrant processes following an error: cognitive to affective to cognitive to affective.

Furthermore, participants may undergo post-error cognitive processing via the caudal ACC through the form of further recognition of his or her error and/or adjustment of his or her response strategy (Falkenstein et al., 2000). Participants may also undergo post-error affective processing via the rostral ACC through the form of an emotional response to his or her error. The possibility of these re-entrant processes is speculative; therefore, further research needs to be conducted in order to draw conclusions.

4.3. Limitations and Future Directions

Although the current study provides useful information in regard to the function of the ACC and lPFC following an error, there are a few limitations to note. First, we were unable to link the fMRI and ERP data on the single-trial level in order to examine these data simultaneously. By examining these on the single-trial level, we might be able to more fully examine variation in timing of when the activation of these regions occurs; therefore, this is an important issue that could be examined in future studies. Second, the present study employed a unimodal, counterbalanced design, rather than attempting simultaneous EEG/fMRI acquisition. Whereas we are unaware of any studies suggesting that the ERN/fMRI signals elicited during error trials vary over time/modality, our design does include the assumption that error trials elicit a canonical, replicable response. Third, the current study only uses one electrode for collection of ERP data and one spatial map in fMRI in the fusion analyses. We selected the Fcz as the ERN was maximal at this location in this data set; however, we recognize that it is likely that electrodes other than Fcz may contribute different information about the ERN. In the future, it would be useful to use all electrodes in order to include topographical ERP components. Fourth, although the current study does provide evidence that a link exists between the ACC and affective error processing, in the future it would be beneficial to further examine whether the ACC is also coupled with autonomic activity. Previous studies have found that autonomic nervous responses can be linked to central processing. Studies involving cognitive and emotional tasks have shown a relationship between rostral ACC and autonomic arousal (Critchley, 2003; Gianaros, 2004). Specifically, errors have been found to actually trigger an autonomic response, suggesting that error processing is directly associated with autonomic arousal (Critchley, 2005; Hajcak, 2003). In the future, we would like to examine the relationship between ACC and autonomic activity with error processing by coupling jICA to fMRI and ERP data. Finally, the current study provides information regarding cognitive and affective function in healthy participants; however, it would be useful to explore if similar results are seen in populations of various psychopathologies. Cognitive and affective dysfunction seems to be evident in many psychopathologies, including but not limited to psychopathy, substance dependence, schizophrenia, and obsessive-compulsive disorder (OCD). More specifically, both divisions of the ACC may play a part in the cognitive and affective dysfunction seen these psychopathologies. When performing working memory tasks, both individuals with psychopathy and substance dependence have shown poorer task performance and decreased caudal and rostral ACC activity compared to control groups (Bolla, 2004; Kiehl, 2001). In addition, these individuals show impairments in emotional processing while symptoms including lack of empathy and shallow affect are evident in individuals with psychopathy (Bolla, 2004; Hare, 1998; Kiehl, 2006). Individuals with schizophrenia and OCD have also shown deficits in ACC activation. Schizophrenia seems to be associated with decreased activation in the caudal and rostral ACC while OCD seems to be associated with increased activation in both divisions (Yucel, 2003). More specifically, Yucel and colleagues suggest that the decreased ACC activity seen in individuals with schizophrenia may lead to impaired goal-directed behavior while the increased ACC activity seen in individuals with OCD may result in excessive goal-directed behavior (Yucel, 2003). In the future, it would be interesting to further explore ACC function in error processing in regard to these different psychopathologies and whether cognition or affect comes first.

Supplementary Material

Refer to Web version on PubMed Central for supplementary material.

Acknowledgments

The research was funded by NIMH 1 R01 MH070539-01 (PI: Kiehl), 1 R01 MH071896-01 (PI: Kiehl), 1R01EB006841 (PI: Calhoun), R01EB005846 (PI: Calhoun), and 5P20RR021938 (PI: Calhoun). We would like to thank Mr. Prashanth Nyalakanti for his help with data analysis support and the individuals who participated in this study.

References

Badgaiyan RD, Posner MI. Mapping the cingulate cortex in response selection and monitoring. NeuroImage. 1998; 7:255–260. [PubMed: 9597666]

Bernstein PS, Scheffers MK, Coles MGH. "Where did I go wrong?" A psychophysiological analysis of error detection. Journal of Experimental Psychology: Human Perception and Performance. 1995; 21:1312–1322. [PubMed: 7490583]

Bolla K, Ernst M, Kiehl K, Mouratidis M, Eldreth D, Contoreggi C, Matochik J, Kurian V, Cadet J, Kimes A, Funderburk F, London E. Prefrontal cortical dysfunction in abstinent cocaine abusers. Journal of Neuropsychiatry and Clinical Neurosciences. 2004; 16:456–464. [PubMed: 15616172]

Botvinick MM, Cohen JD, Carter CS. Conflict monitoring and anterior cingulate cortex: An update. Trends in Cognitive Sciences. 2004; 8:539–546. [PubMed: 15556023]

Botvinick MW, Carter CS, Braver TS, Barch DM, Cohen JD. Conflict monitoring and cognitive control. Psychological Review. 2001; 108:624–652. [PubMed: 11488380]

Braver TS, Barch DM, Gray JR, Molfese DL, Snyder A. Anterior cingulate cortex and response conflict: Effects of frequency, inhibition, and errors. Cerebral Cortex. 2001; 11:825–836. [PubMed: 11532888]

Brown JW, Braver TS. Learned predictions of error likelihood in the anterior cingulate cortex. Science. 2005; 307:1118–1121. [PubMed: 15718473]

Bush G, Luu P, Posner MI. Cognitive and emotional influences in anterior cingulate cortex. Trends in Cognitive Sciences. 2000; 4:215–222. [PubMed: 10827444]

Calhoun VD, Adali T, Pearlson GD, Kiehl KA. Neuronal chronometry of target detection: Fusion of hemodynamic and event-related potential data. NeuroImage. 2006; 30:544–553. [PubMed: 16246587]

Calhoun VD, Adali T, Pearlson GD, Pekar JJ. A method for making group inferences from functional MRI data using independent component analysis. Human Brain Mapping. 2001; 14:140–151. [PubMed: 11559959]

Calhoun VD, Liu J, Adali T. A review of group ICA for fMRI data and ICA for joint inference of imaging, genetic, and ERP data. NeuroImage. 2009; 45:163–172.

Carter CS, Botvinick MM, Cohen JD. The contribution of the anterior cingulate cortex to executive processes in cognition. Reviews in the Neurosciences. 1999; 10:49–57. [PubMed: 10356991]

Carter CS, Braver TS, Barch DM, Botvinick MM, Noll D, Cohen JD. Anterior cingulate cortex, error detection, and the online monitoring of performance. Science. 1998; 280:747–749. [PubMed: 9563953]

Casey BJ, Thomas KM, Welsh TF, Badgaiyan RD, Eccard CH, Jennings JR, Crone EA. Dissociation of response conflict, attentional selection, and expectancy with functional magnetic resonance imaging. Proceedings of the National Academy of Sciences. 2000; 97:8728–8733.

Cohen D, Cuffin N, Yunokuchi K, Maniewski R, Purcell C, Cosgrove GR, Ives J, Kennedy JG, Schomer DL. MEG versus EEG localization test using implanted sources in the human brain. Annals of Neurology. 1990; 28:811–817. [PubMed: 2285267]

Coles, MGH.; Scheffers, MK.; Holroyd, C. Error-related brain activity: Historical introduction. Denver, CO: Society for Psychophysiological Research; 1998.

Critchley HD, Mathias CJ, Josephs O, O'Doherty J, Zanini S, Dewar BK, Cipolotti L, Shallice T, Dolan RJ. Human cingulate cortex and autonomic control, converging neuroimaging and clinical evidence. Brain. 2003; 126:2139–2152. [PubMed: 12821513]

Critchley HD, Tang J, Glaser D, Butterworth B, Dolan RJ. Anterior cingulate activity during error and autonomic response. NeuroImage. 2005; 27:885–895. [PubMed: 15996878]

Debener S, Ullsperger M, Siegel M, Fiehler K, Yves von Cramen D, Engel AK. Trial-by-trial coupling of concurrent electoenceplalogram and functional magnetic resonance imaging identifies the dynamics of perfomance monitoring. The Journal of Neuroscience. 2005; 25:11730–11737. [PubMed: 16354931]

Dehaene S, Posner MI, Tucker DM. Localization of a neural system for error detection and compensation. American Psychological Society. 1994; 5:303–305.

Devinsky O, Morrell MJ, Vogt BA. Contributions of anterior cingulate to behaviour. Brain. 1995; 118:279–306. [PubMed: 7895011]

Downar J, Crawley AP, Mikulis DJ, Davis KD. A cortical network sensitive to salience in a neutral behavioral context across multiple sensory modalities. Journal of Neurophysiology. 2002; 87:615–620. [PubMed: 11784775]

Drevets WC, Raichle ME. Recipricol suppression of regional cerebral blood flow during emotional versus higher cognitive processes: Implications for interactions between emotion and cognition. Cognition and Emotion. 1998; 12:353–385.

Falkenstein M, Hohnsbein J, Hoormann J, Blanke L. Effects of crossmodal divided attention on late ERP components: II. Error processing in choice reaction tasks. Electroencephalophagraphy and Clinical Neurophysiology. 1991; 78:447–455.

Falkenstein M, Hoormann J, Christ S, Hohnsbein J. ERP components on reaction errors and their functional significance: A tutorial. Biological Psychology. 2000; 51:87–107. [PubMed: 10686361]

Freire L, Roche A, Mangin JF. What is the best similarity measure for motion correction in FMRI time series? IEEE Transactions on Medical Imaging. 2002; 21:470–484. [PubMed: 12071618]

Friston K, Ashburner J, Frith CD, Poline JP, Heather JD, Frackowiak RS. Spatial registration and normalization of images. Human Brain Mapping. 1995; 2:165–189.

Garavan H, Ross TJ, Kaufman J, Stein EA. A midline dissociation between error-processing and response-conflict monitoring. NeuroImage. 2003; 20:1132–1139. [PubMed: 14568482]

Gehring WJ, Coles MGH, Meyer DE, Donchin E. The error-related negativity: An event-related brain potential accompanying errors. Psychophysiology. 1990; 27:S43.

Gehring WJ, Fencsik DE. Functions of the Medial Frontal Cortex in the Processing of Conflict and Errors. The Journal of Neuroscience. 2001; 21:9430–9437. [PubMed: 11717376]

Gehring WJ, Goss B, Coles MGH, Meyer DE, Donchin E. A neural system for error detection and compensation. Psychological Science. 1993; 4:385–390.

Gianaros PJ, Van Der Veen FM, Jennings JR. Regional cerebral blood flow correlates with heart period and high-frequency heart period variability during working-memory tasks: implications for the cortical and subcortical regulation of cardiac autonomic activity. Psychophysiology. 2004; 41:521–530. [PubMed: 15189475]

Hajcak G, McDonald N, Simons RF. To err is autonomic: Error-related brain potentials, ANS activity, and post-error compensatory behavior. Psychophysiology. 2003; 40:895–903. [PubMed: 14986842]

Hajcak G, Moser JS, Yeung N, Simons RF. On the ERN and the significance of errors. Psychophysiology. 2005; 42:151–160. [PubMed: 15787852]

Hare, RD. Psychopathy, affect, and behavior. Kluwer: Dordrecht; 1998.

Herrmann MJ, Rommler J, Ehlis A, Heidrich A, Fallgatter AJ. Source localization (LORETA) of the error-related-negativity (ERN/Ne) and positivity (Pe). Cognitive Brain Research. 2004; 20:294–299. [PubMed: 15183400]

Holroyd CB, Nieuwenhuis S, Yeung N, Nystrom L, Mars RB, Coles MGH, Cohen JD. Dorsal anterior cingulate cortex shows fMRI response to internal and external error signals. Nature Neuroscience. 2004; 7:497–498.

Jung TP, Makeig S, Humphries C, Lee TW, McKeown MJ, Iragui V, Sejnowski TJ. Removing electroencephalographic artifacts by blind source separation. Psychophysiology. 2000; 37:163–178. [PubMed: 10731767]

Kiehl KA. A cognitive neuroscience perspective on psychopathy: Evidence for paralimbic system dysfunction. Psychiatry Research. 2006; 142:107–128. [PubMed: 16712954]

Kiehl KA, Liddle PF, Hopfinger JB. Error processing and the rostral anterior cingulate: An event-related fMRI study. Psychophysiology. 2000; 37:216–223. [PubMed: 10731771]

Kiehl KA, Smith AM, Hare RD, Mendrek A, Forster BB, Brink J, Liddle PF. Limbic abnormalities in affective processing by criminal psychopaths as revealed by functional magnetic resonance imaging. Biological Psychiatry. 2001; 50:677–684. [PubMed: 11704074]

Logan GD. Executive control of thought and action. Special issue: Action, attention, and automaticity. Acta Psychologica. 1985; 60:193–210.

Luu P, Tucker DM, Derryberry D, Reed M, Poulsen C. Electrophysiological Responses to Errors and Feedback in the Process of Action Regulation. Psychological Science. 2003; 14:47–53. [PubMed: 12564753]

Nieuwenhuis S, Ridderinkhof KR, Blom J, Band GPH, Kok A. Error-related brain potentials are differentially related to awareness of response errors: Evidence from an antisaccade task. Psychophysiology. 2001; 38:752–760. [PubMed: 11577898]

Polli FE, Wright CI, Milad MR, Dickerson BC, Vangel M, Barton JJS, Rauch SL, Manoach DS. Hemispheric differences in amygdala contributions to response monitoring. NeuroReport. 2009; 20:398–402. [PubMed: 19218865]

Roger C, Benar CG, Vidal F, Hasbroucq T, Burle B. Rostral Cingulate Zone and correct response monitoring: ICA and source localization evidences for the unicity of correct- and error-negativities. NeuroImage. 2010; 51:391–403. [PubMed: 20152906]

Ruff CC, Woodward TS, Laurens KR, Liddle PF. The role of the anterior cingulate cortex in conflict processing: Evidence from reverse stroop interference. . NeuroImage. 2001; 14:1150–1158. [PubMed: 11697946]

Shallice, T. From neuropsychology to mental structure. New York: Cambridge University Press; 1988.

Srinivasan R. Methods to improve the spatial resolution of EEG. International Journal of Bioelectromagnetism. 1999; 1:102–111.

Stuss, DT.; Alexander, MP.; Benson, DF., editors. Frontal lobe functions. Boston: Butterworth-Heinemann; 1997.

Swick D, Turken AU. Dissociation between conflict detection and error monitoring in the human anterior cingulate cortex. PNAS. 2002; 99:16354–16359. [PubMed: 12456882]

Ullsperger M, Yves von Cramon D. Subprocesses of performance monitoring: A dissociation of error processing and response competition revealed by event-related fMRI and ERPs. NeuroImage. 2001; 14:1387–1401. [PubMed: 11707094]

Vogt BA. Pain and emotion interactions in subregions of the cingulate gyrus. Nature Reviews Neuroscience. 2005; 6:533–544.

Vogt BA, Finch DM, Olson CR. Functional heterogeneity in cingulate cortex: The anterior executive and posterior evaluative regions. Cerebral Cortex. 1992; 2:435–443. [PubMed: 1477524]

Whalen PJ, Bush G, McNally RJ, Wilhelm S, McInerney SC, Jenike MA, Rauch SL. The emotional counting stroop paradigm: A functional magnetic resonance imaging probe of the anterior cingulate affective division. Society of Biological Psychiatry. 1998; 44:1219–1228.

Yucel M, Wood SJ, Fornito A, Riffkin J, Velakoulis D, Pantelis C. Anterior cingulate dysfunction: Implications for psychiatric disorders? Journal of Psychiatry and Neuroscience. 2003; 28:350–354. [PubMed: 14517578]

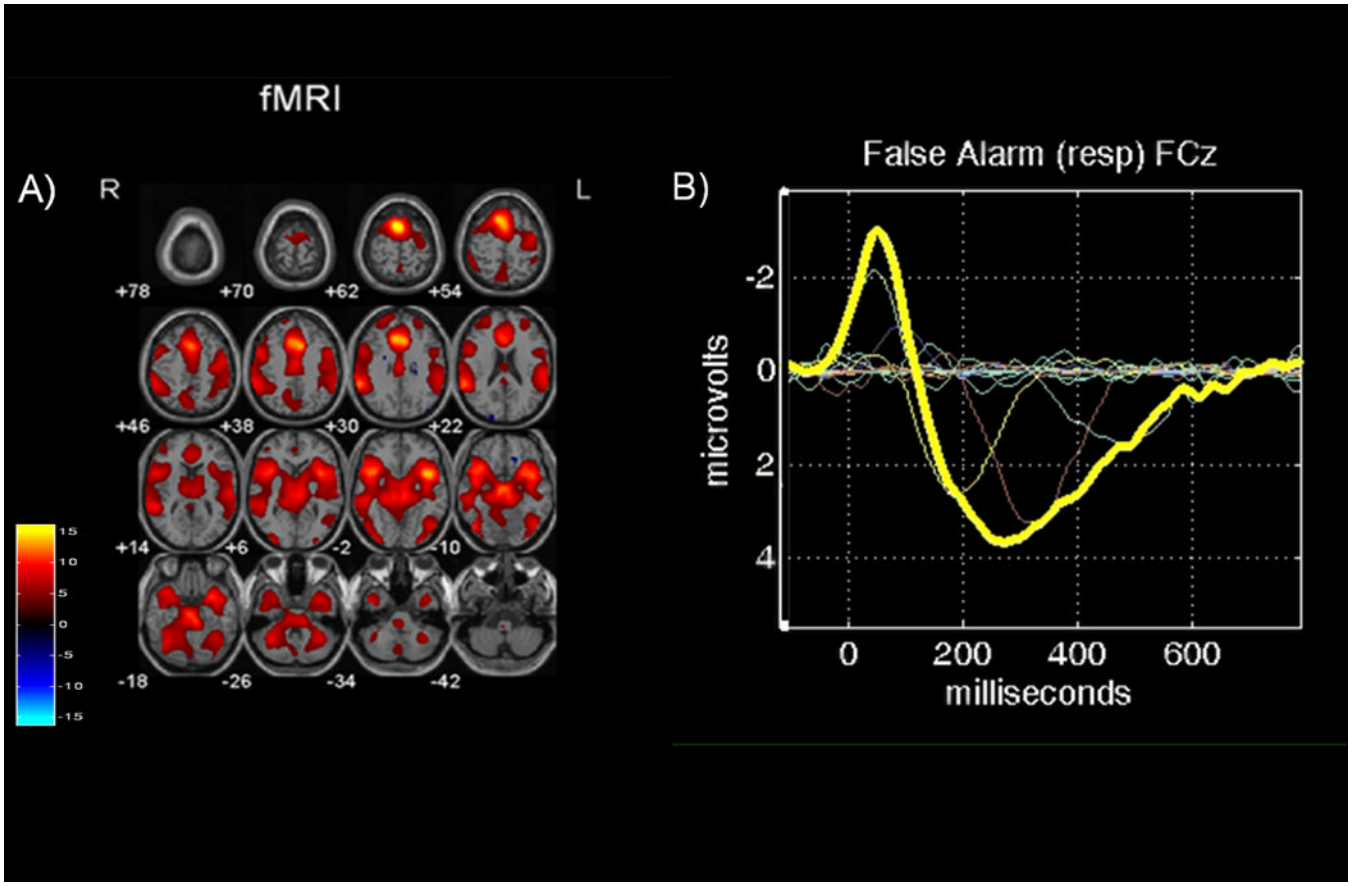

Figure 1.
fMRI (A) and ERP (B) results averaged across subjects for false alarms relative to pre-stimulus baseline. Averaged ERP time course in yellow and estimated ERP components are shown on the right. Positive (orange) and negative (blue) Z values are shown in the images. In the fMRI map, left is right and right is left.

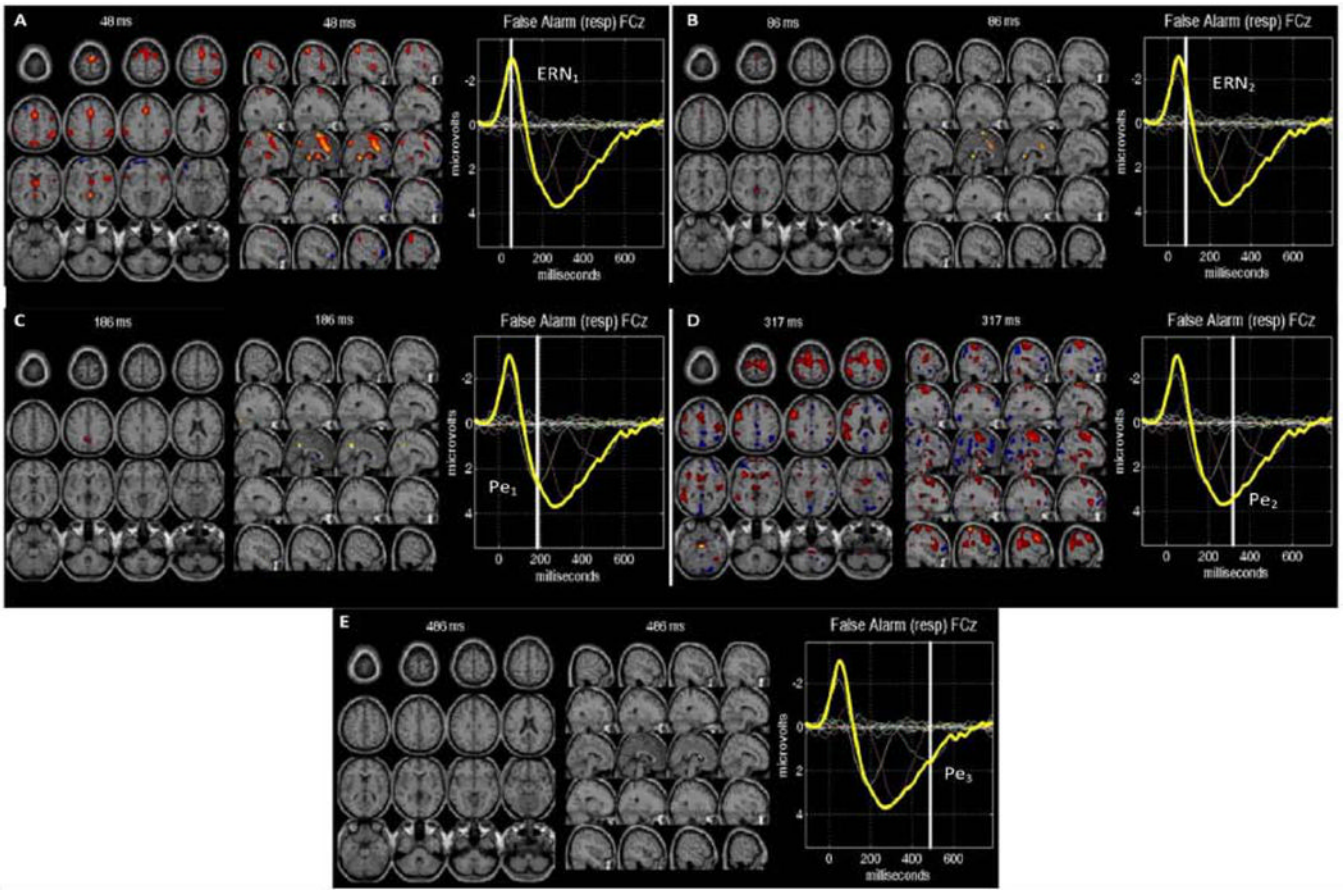

Figure 2.

A–E. Combination of fMRI and ERP data for false alarms using ICA. Five compounds were found to significantly load onto the ERP time courses. ERP compounds and fMRI maps are shown in “snapshots”. fMRI maps are weighted by the ERP part of the component at a specific point in these (highlighted by white line in ERP graph) are shown on the left. Average ERP time course in yellow and estimated ERP components are shown on the right. Positive (orange) and negative (blue) Z values are shown in the images. In regards to the fMRI maps, left is right and right is left.

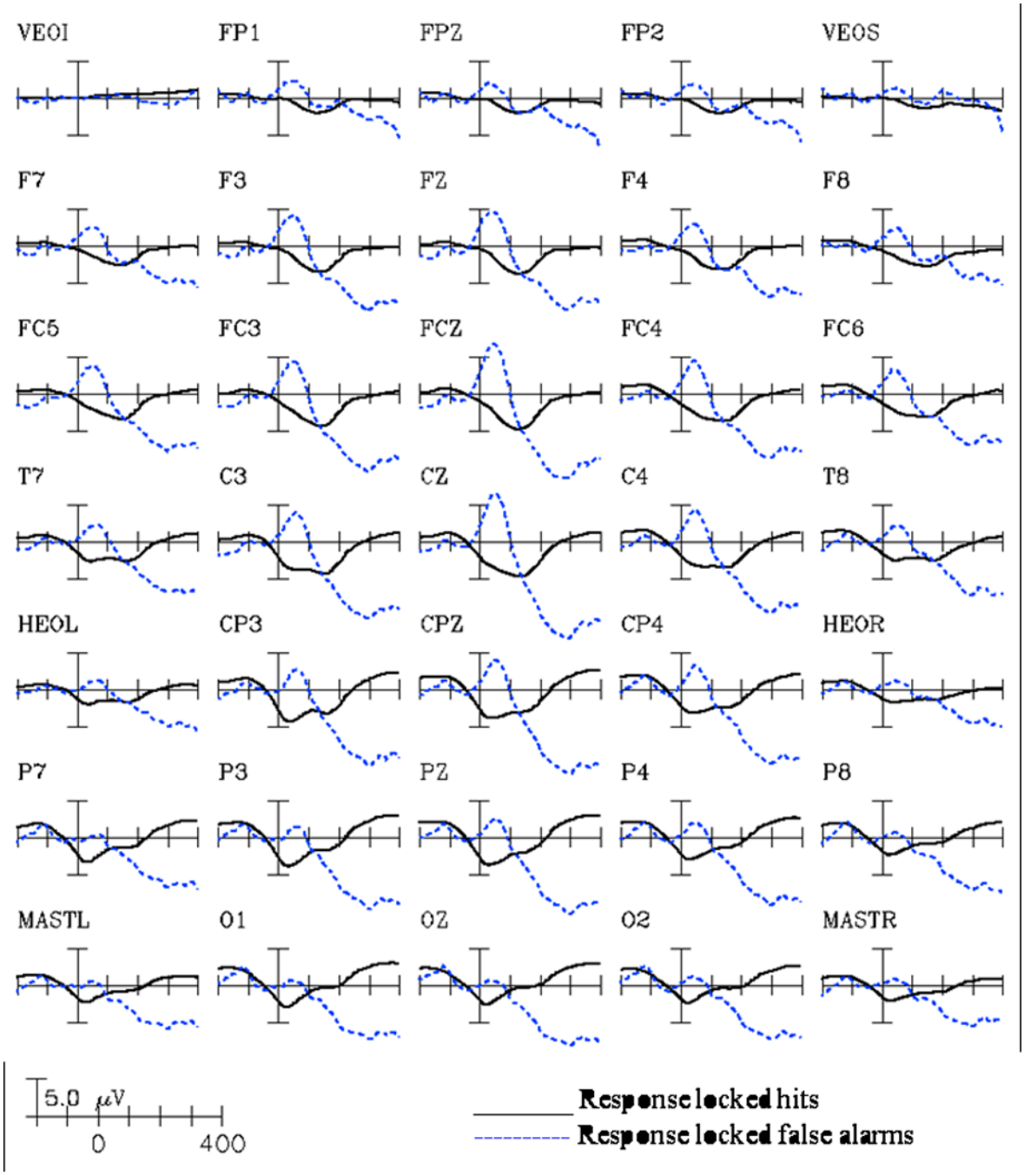

Figure 3.

Table 1

Behavioral results by session.

	ERP Session Mean (SD)	fMRI Session Mean (SD)
Correct Rejects	54.39 (11.00)	49.90 (12.58)
Hits	413.07 (18.57)	407.12 (12.63)
Hits RT	375.24 (49.16)	398.05 (62.26)
False Alarms	24.12 (11.15)	28.10 (12.58)
False Alarms RT	339.57 (52.64)	352.97 (40.44)

Table 2

Anterior cingulate activation associated with event-related potentials.

			MNI Coordinates			
Region	**Brodmann Area**	**Volume (cc)**	**X**	**Y**	**Z**	**Max T**
ERN_1 Component						
Caudal Anterior Cingulate	24	1.3	+0	+24	+27	6.5^{***}
Caudal Anterior Cingulate	24	0.9	+3	+27	+27	6.1^{***}
ERN_2 Component						
Rostral Anterior Cingulate	32	0.5	−3	+42	−3	4.1^{**}
Rostral Anterior Cingulate	25	0.6	+0	+3	+0	6.6^{***}
Rostral Anterior Cingulate	25	0.3	+3	+6	−3	5.3^{***}
Pe_1 Component						
Caudal Anterior Cingulate	24	0.3	+0	+27	+24	4.2^{***}
Caudal Anterior Cingulate	24	0.1	+3	+27	+27	3.6^{**}
Rostral Anterior Cingulate	25	0.2	+0	+9	+0	4.1^{**}
Rostral Anterior Cingulate	32	0.1	+9	+33	−12	3.4^{*}
Pe_2 Component						
Caudal Anterior Cingulate	24	0.2	+0	+24	+24	3.6^{**}
Caudal Anterior Cingulate	24	0.1	+3	+30	+21	3.4^{*}
Pe_3 Component						
Rostral Anterior Cingulate	24	1.8	+0	+24	+3	6.5^{***}

X, Y, and Z depict coordinates in the standard Montreal Neurological Institute (MNI) space. Selected MNI coordinates of the volume and maxima of each anatomic region within the maps are presented.

* $p \leq .01$,

** $p \leq .001$,

*** $p \leq .0001$.

Table 3

Activation associated with ERN and Pe components of event-related potentials.

			MNI Coordinates			
Region	**Brodmann Area**	**Volume (cc)**	**X**	**Y**	**Z**	**Max T**
ERN_1 Component						
Caudal Anterior Cingulate	24	1.3	+0	+24	+27	6.5***
Caudal Anterior Cingulate	24	0.9	+3	+27	+27	6.1***
Left Middle Frontal Gyrus	6	1.7	−36	+0	+66	4.9***
Right Middle Frontal Gyrus	6	4.4	+45	+0	+54	5.2***
ERN_2 Component						
Left Middle Frontal Gyrus	10	7.1	−33	+60	+3	6.8***
Rostral Anterior Cingulate	32	0.5	−3	+42	−3	4.1**
Rostral Anterior Cingulate	25	0.6	+0	+3	+0	6.6***
Rostral Anterior Cingulate	25	0.3	+3	+6	−3	5.3***
Pe_1 Component						
Caudal Anterior Cingulate	24	0.3	+0	+27	+24	4.2***
Caudal Anterior Cingulate	24	0.1	+3	+27	+27	3.6**
Left Middle Frontal Gyrus	10	1.9	−30	+66	+12	6.4***
Left Superior Frontal Gyrus	10	3.0	−27	+66	+15	6.0***
Right Middle Frontal Gyrus	10	0.4	+24	+60	+27	5.4***
Right Superior Frontal Gyrus	10	1.4	+21	+63	+27	5.2***
Rostral Anterior Cingulate	25	0.2	+0	+9	+0	4.1**
Rostral Anterior Cingulate	32	0.1	+9	+33	−12	3.4*
Pe_2 Component						
Caudal Anterior Cingulate	24	0.2	+0	+24	+24	3.6**
Caudal Anterior Cingulate	24	0.1	+3	+30	+21	3.4*
Left Middle Frontal Gyrus	9	7.3	−51	+15	+33	6.5***
Left Superior Frontal Gyrus	6	5.9	−9	+9	+69	6.5***

			MNI Coordinates			
Region	**Brodmann Area**	**Volume (cc)**	**X**	**Y**	**Z**	**Max T**
Right Middle Frontal Gyrus	6	1.2	+33	−6	+66	5.6***
Right Superior Frontal Gyrus	6	1.8	+18	−15	+78	6.3***
Pe_3 Component						
Left Middle Frontal Gyrus	47	0.6	−48	+36	−6	4.9***
Left Superior Frontal Gyrus	6	1.5	−3	+3	+72	4.0**
Right Middle Frontal Gyrus	11	0.5	+42	+42	−15	3.8**
Right Superior Frontal Gyrus	10	0.1	+21	+57	−9	3.5**
Rostral Anterior Cingulate	24	1.8	+0	+24	+3	6.5***

X, Y, and Z depict coordinates in the standard Montreal Neurological Institute (MNI) space. Selected MNI coordinates of the volume and maxima of each anatomic region within the maps are presented.

* $p \leq .01$,

** $p \leq .001$,

*** $p \leq .0001$.